Facile Construction of New Hybrid Conjugation *via* Boron Cage Extension

Fangxiang Sun[1], Shuaimin Tan[1], Hou-Ji Cao[5], Changsheng Lu[1], Deshuang Tu[1]*, Jordi Poater[2, 3]*, Miquel Solà[4]*, Hong Yan[1]*

[1]State Key Laboratory of Coordination Chemistry, Jiangsu Key Laboratory of Advanced Organic Materials, School of Chemistry and Chemical Engineering, Nanjing University, Nanjing 210023, China.

[2]Departament de Química Inorgànica i Orgànica & IQTCUB, Universitat de Barcelona, Martí i Franquès 1-11, Barcelona 08028, Spain.

[3]ICREA, Pg. Lluís Companys 23, Barcelona 08010, Spain.

[4]Institut de Química Computacional i Catàlisi and Departament de Química, Universitat de Girona, C/ Maria Aurèlia Capmany, 69, Girona 17003, Catalonia, Spain.

[5]School of Chemistry and Chemical Engineering, Henan Normal University, XinXiang, Henan 453007, China.

ABSTRACT: Aromatic polycyclic systems have been extensively utilized as structural subunits for the preparation of various functional molecules. Currently, aromatics-based polycyclic systems are predominantly generated from the extension of two-dimensional (2D) aromatic rings. By contrast, polycyclic compounds based on the extension of three-dimensional (3D) aromatics such as boron clusters are less studied. Here we report three types of boron cluster-cored tricyclic molecular systems which are constructed from a 2D aromatic ring, a 3D aromatic *nido*-carborane and an alkyne. These new tricyclic compounds could be facilely accessed by Pd-catalyzed B–H activation and the subsequent cascade heteroannulation of carborane and pyridine with an alkyne in an isolated yield of up to 85% under mild conditions without any additives. Computational results indicate that the newly generated ring from the fusion of the 3D carborane, the 2D pyridyl ring, and an alkyne is non-aromatic. However, such fusion not only leads to ^{1}H chemical shift considerably downfield shifted owing to the strong diatropic ring current of the embedded carborane, but also devotes to new/improved physicochemical properties including increased thermal stability, the emergence of a new absorption band, as well as a largely red-shifted emission band and enhanced emission efficiency. Besides, a number of bright, color-tunable solid emitters spanning over all visible light are obtained with absolute luminescence efficiency of up to 61%, in contrast to aggregation-caused emission quenching of *Rhodamine B* containing a 2D-aromatics fused structure. This work demonstrates that the new hybrid conjugated tricyclic systems might be promising structural scaffolds for the construction of functional molecules.

INTRODUCTION

Polycyclic compounds are important molecular systems in fundamental research and applications.[1–6] To date, tremendous amounts of polycyclics with intriguing properties,[7–9] for example, graphene, are constructed by the extension of aromatics (Figure 1a). These have inspired us to explore new strategies for the construction of polycyclics and further investigate their structures and properties, as well as their applications.

At difference to two-dimensional (2D) aromatic rings, boron clusters like carboranes possess three-dimensional (3D) aromaticity,[10–14] which include multiple B–H and/or C–H bonds (Figure 1b). Both cage-type molecular structures and multi-center multi-electron bonding characteristics of boron clusters endow them with unique properties such as 3D aromaticity, rigid geometry, high thermal and chemical stability, low toxicity, bulky size, and hydrophobicity. All these properties make them and their derivatives attractive for a wide variety of applications in various fields from medicine to materials science. As such, carboranes have been utilized as important building blocks to construct functional molecules[15–34] and tunable pharmacophores (especially for Boron Neutron Capture Therapy (BNCT) drugs).[35–48] Among these studies, carboranes are generally treated as an "appended" structural unit. However, it would be more interesting and distinct if carborane-embedded polycyclic systems would be developed with carborane playing a central role. In such a way, the carborane together with the extended part could serve as a new and united structural skeleton.[49–53] So far, such a "cage extension strategy" to construct boron cluster-cored polycyclics is much less established in contrast to the classical extension of 2D aromatic rings.

Herein we designed and prepared a new hybrid conjugated system, i.e. fusion between a 2D aromatic ring and a 3D *nido*-carborane (Figure 1b) by facile Pd-catalyzed B–H activation and subsequent cascade heteroannulation of carborane and pyridine with alkynes. By using this reaction protocol of cage extension, three types of fused skeletons have been generated in high yields under mild conditions without any additives (Figure 1b). These boron cluster fused systems demonstrate distinct properties such as enhanced chemical and thermal stability, tunable emission behaviors, and highly efficient solid-state emission, in contrast to the control compounds like 2D aromatic rings-based polycyclics or non-fused boron cluster systems. Thus, these hybrid fused molecular systems not only extend the scope of aromatics-based polycyclics but also show potential applications in luminescent materials, drugs, and other related fields.

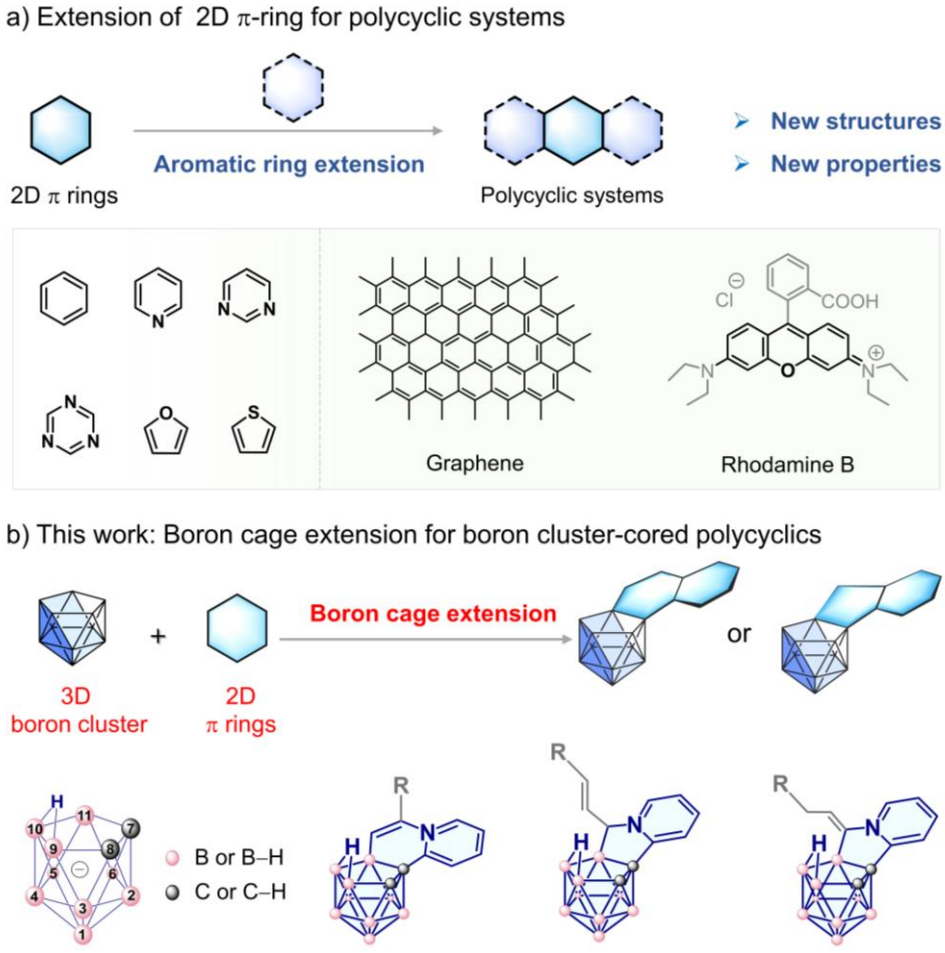

Figure 1. a) The extension of 2D aromatic rings to construct polycyclic ring systems. The selected examples are the classical 2D aromatic rings (left) and 2D aromatics-based polycyclic systems (right). b) The boron cage extension for 3D carborane-based tricyclic systems, i.e., the fusion between a 2D aromatic ring and a 3D *nido*-carborane by an alkyne. The three types of carborane-based tricyclics are zwitterions, with the positive charge located on the pyridyl group.

RESULTS AND DISCUSSION

Construction of boron cluster-cored tricyclics *via* cage extension. Since the discovery of carboranes in the last century, their functionalization has been the central study in boron chemistry. In particular, the 3D cage structure of carboranes containing multiple B–H vertexes allows them to be substituted by various functional groups to construct B–C or B–X (X = heteroatoms) bonds.[54–59] In recent years, the fast development of B–H functionalization has offered an alternative and efficient pathway to synthesize the functionalized carborane derivatives.[60–80] However, it remains challenging to use these known synthetic schemes to readily access the aforementioned 2D-3D fused molecular systems as the following issues have to be addressed: I) Site-selective functionalization among the multiple B–H/C–H bonds; II) Realization of stepwise reactions in a one-pot manner; III) The steric hindrance effect of 3D carborane; IV) The side reactions associated with the B–H functionalization.

To tackle the above issues and obtain a library of boron cluster-based polycyclics, here a new reaction protocol, i.e. directing group-assisted, metal-catalyzed B–H activation of *nido*-carboranes and cascade cyclization was considered. We selected (NMe_3H)(7-pyridyl-*nido*-$C_2B_9H_{11}$) (**1a**) as the starting material as the pyridyl directing group is capable of lowering the reaction barrier and controlling the site selectivity,[81] but also serving as the aromatic N-heterocyclics for building the fused tricyclic molecular system (Figure 1b and Tables 1–3). The alkyne **2aa** (1-ethynyl-4-methoxybenzene) was utilized as the coupling partner to evaluate the feasibility of the above proposed synthetic strategy. By screening different catalysts, solvents, and temperatures, we obtained the best reaction conditions: **1a** and **2aa** in the presence of $Pd(OAc)_2$ in dichloroethane (DCE) under the argon atmosphere at 40 °C for 3 hours to afford the carborane-based tricyclic compound **3a** in an isolated yield of 78% (see Table S1 for details). In addition, a slightly lower yield was observed if this reaction was performed in air (Table S1, entry 14). In the absence of a Pd-catalyst, no product was generated (Table S1, entry 15). If **1a** was replaced by 2-phenylpyridine, no reaction occurred.

With the optimal reaction conditions in hand, the substrate scope of alkynes was examined. We were pleased to find that many alkynes could react with **1a** smoothly to generate carborane-fused tricyclic compounds in good isolated yields. As shown in Table 1, the terminal aryl alkynes containing electron-donating groups such as methoxy, amidogen, diphenylaminyl could participate in the B–H activation and further annulation to produce carborane-fused products where a new six-membered ring is incorporated (**3a**–**3f**). Unfortunately, the annulated products could not be generated if the terminal aryl alkynes contained an electron-withdrawing group on the aryl ring, demonstrating that cycle-closing is quite sensitive to the electron density of the carbon of the alkyne connected to the aryl substituent. In addition, the reaction was also compatible with the substrate with an alkyne containing a heterocyclic substituent (**3g**). The internal alkynes bearing less steric hindrance like 1-phenyl-1-propyne could also lead to the expected product (**3h**). In addition, both electron-donating and electron-withdrawing groups on pyridyl rings offered satisfying yields (**3i** and **3j**). By altering the substituent at the cage-carbon site, comparable outcomes were also obtained (**3k**–**3m**). Both electron-donating and electron-withdrawing groups on the phenyl rings of carboranes gave rise to similar yields (**3l** and **3m**). Using 3-chloropropyne as the starting compound, **3n** was isolated as the sole product. When utilizing quinolyl instead of pyridyl as the directing group, we got **3o** bearing

Table 1 Reaction scope I[a]

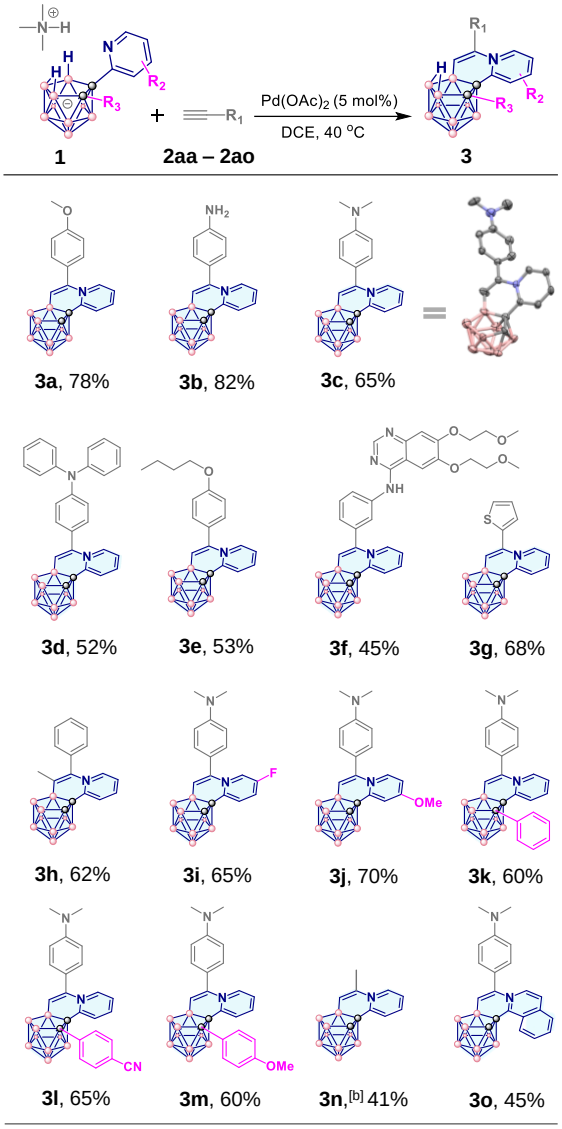

[a]Reaction conditions: **1** (0.1 mmol), **2a** (0.1 mmol), $Pd(OAc)_2$ (5% eq.), DCE (4.0 mL), 40 °C, 3 h, yield of isolated product, unless otherwise noted. The B–H–B bridging proton of **3a**–**3o** is omitted for clarity. [b]The substrate of the alkyne is 3-chloropropyne.

a tetracyclic system. The regioselectivity of the reaction was confirmed by the X-ray crystallography, as the crystal structure of **3c** showed (Table 1). If an alkyne bearing an α-OH was used, we obtained the carborane-cored tricyclics containing a new five-membered ring, instead of a six-membered ring, of which only one carbon atom from the alkyne is involved in its formation (Tables 2 and 3). If R_1 = aryl, R_2 = H, the carborane-fused products (**4a**–**4k**) were synthesized where the sp^2-hybrid carbon originated from the terminal sp carbon of alkyne is incorporated in the five-membered ring, as confirmed by NMR data and crystal structures (Table 2). Here, the newly generated CH_2–CH=C unit demonstrates interesting coupling patterns for the two methylene hydrogen atoms with the coupling constants of 14.8 Hz from each other and 8.0 Hz from the adjacent olefinic CH.

Table 2 Reaction scope II[a]

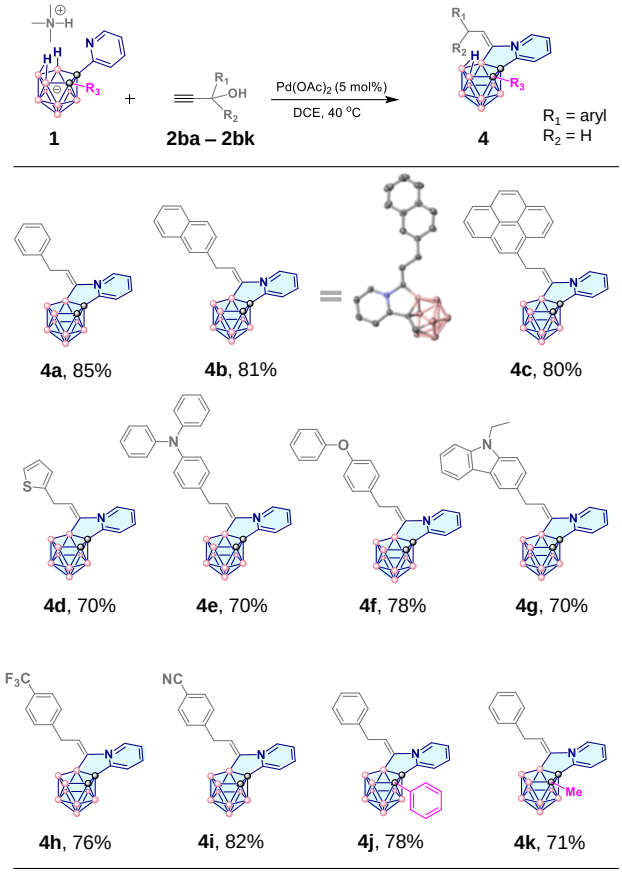

[a]Reaction conditions: **1** (0.1 mmol), **2b** (0.1 mmol), $Pd(OAc)_2$ (5% eq.), DCE (4.0 mL), 40 °C, 3 h, yield of isolated product, unless otherwise noted. The B–H–B bridging proton of **4a**–**4k** is omitted for clarity.

Notably, no effect from the size of the aryl group of the alkyne on reaction yield was observed (**4a**–**4c**). The reaction was also compatible with a heteroaromatic ring (**4d**). Both electron-donating and electron-withdrawing groups on the aryl rings of the alkynes offered similar yields (**4e**–**4i**). By attaching methyl or phenyl at the cage-carbon site, comparable outcomes were also generated (**4j** and **4k**), demonstrating that the substitution at the cage-carbon site has a negligible effect on the reaction yield. Interestingly, if R_1 = alkyl, R_2 = alkyl/H or R_1/R_2 = aryl, the carborane-based tricyclic compounds were obtained where a sp^3-hybrid carbon originating from the alkyne is inserted in the new five-membered ring (**5a**–**5q**) under the same reaction conditions (Table 3). If the terminal alkynes have both alkyl substituents or alkyl/H at the α carbon, the products **5a**–**5j** were obtained in good yields. Here the size of the alkyl substituent has little effect on reaction yield. Additionally, late-stage carboranylation of drug molecules and natural products such as camphor, ethisterone, and perilla aldehyde gave rise to the products (**5g**–**5i**) by the reaction with corresponding alkyne precursor. If the alkynes bearing two aryl groups at the α carbon site were utilized, products **5k**–**5p** were generated. Both electron-donating and electron-withdrawing groups on aryl rings did not affect reaction yield. When the mixed-type R_1 and R_2 such as methyl and phenyl were selected, product **5q** in *E*-form was generated as confirmed by NMR data and X-ray crystallography.

Table 3 Reaction scope III[a]

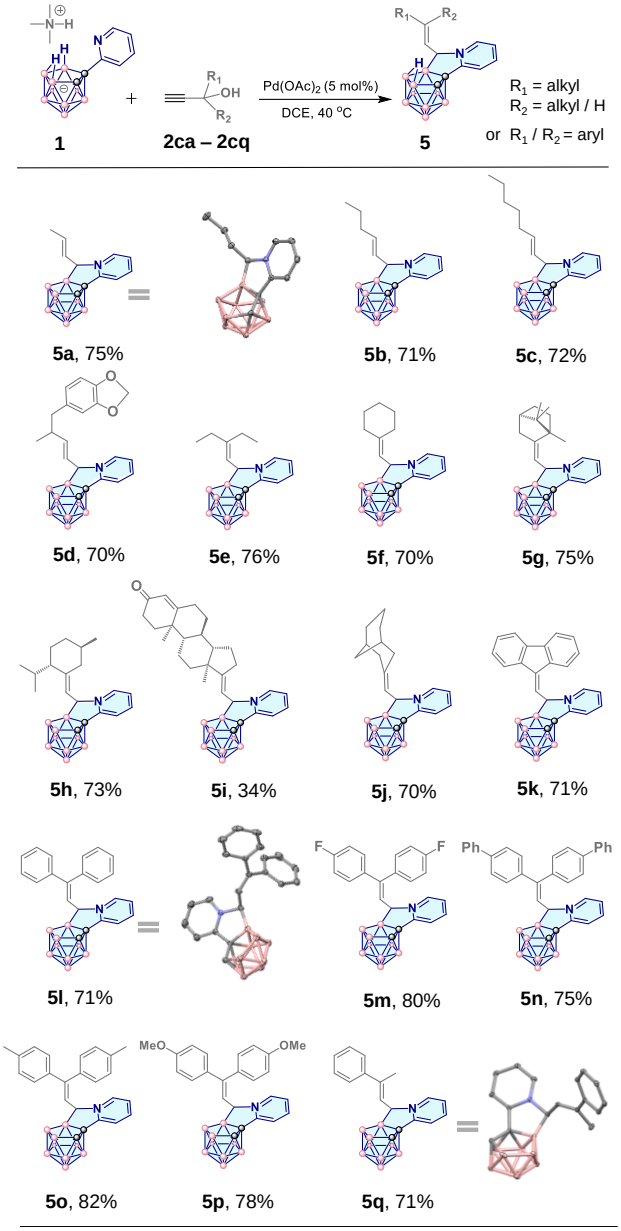

[a]Reaction conditions: **1** (0.1 mmol), **2c** (0.1 mmol), $Pd(OAc)_2$ (5% eq.), DCE (4.0 mL), 40 °C, 3 h, isolated yield, unless otherwise noted. The B–H–B bridging proton of **5a**–**5q** is omitted for clarity.

The structures of all the new carborane derivatives were characterized by ^1H, ^{13}C, and ^{11}B nuclear magnetic resonance (NMR) and high-resolution mass spectrometry (HRMS), among which **3c**, **3n**, **4b**, **5a**, **5l**, and **5q** were unambiguously identified by single-crystal X-ray diffraction. Overall, three types of boron cluster-cored tricyclics are obtained in a one-pot reaction. Here the synthetic methodology of boron cage extension represents a brand-new strategy for the construction of different carborane-cored polycyclics through control of the type of alkynes used.

Mechanistic investigations. According to our previous work[65] and literature,[82–88] plausible mechanisms were proposed and validated by gas chromatography (GC), NMR, and HRMS technologies (Figures S10–S19). For the five-membered ring products, after the

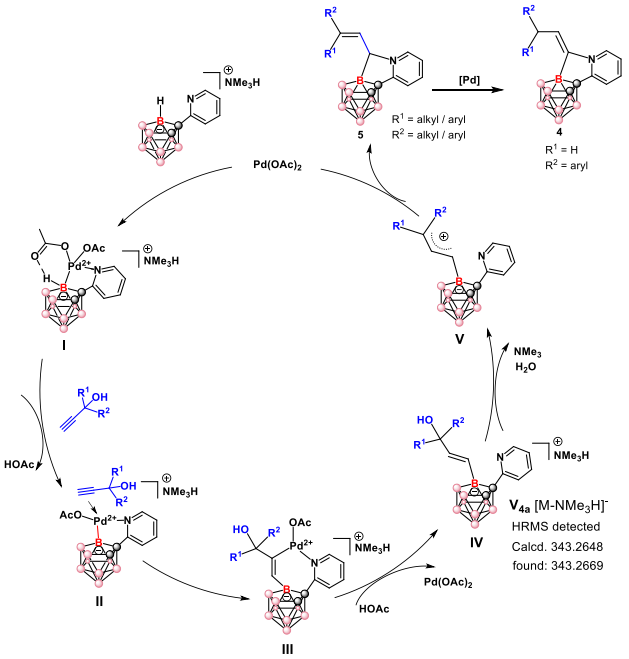

Figure 2. Proposed reaction mechanism for five-membered ring products **4** and **5**. The B–H–B bridging proton is omitted for clarity.

coordination of pyridyl to metal (i.e. Pd(II)), the selective B–H activation and regioselective alkyne insertion into Pd–B bond occurs sequentially to lead to intermediate **III**, which further proceeds proto-demetalation to generate **IV**. This species has been detected by HRMS (Figures S18 and S19). Such type of structure could be isolated if internal aryl alkyne substrates were used.[65] Then dehydration leads to the allyl cation (**V**). Finally, the nucleophilic attack of the N atom of pyridyl gives rise to the five-membered ring products **5**, which could rearrange to yield products **4** dependent on the type of alkynes under the reaction conditions (Figure 2). The C=C bond immigration has been detected by continuous tracking of the ^{1}H NMR (Figure S13). In the case of the formation of six-membered ring products of **3**, similar procedures proceed until the formation of intermediate **III** in Figure 2 (see Figure S12), from which reductive elimination, rather than proto-demetalation, takes place to lead to the ring-closing. The type of products is determined by the alkyne used.

Structural insights into boron cluster-cored tricyclics. To gain structural insights into the above new fused structures, the selected crystal structures of **3n**, **4b**, **5a** (Figures 3a–3c) and the non-fused control crystal structures of ***nido*-1** (Figure 3d) and ***nido*-2** (Figure S8) were studied. The carborane cage is indeed fused with the pyridyl ring by sharing the middle six- or five-membered ring to generate completely new conjugated systems. But they present a non-planar geometry, which is distinct from the 2D fused rings like planar phenanthrene. The dihedral angles between the C_2B_3 face (plane A) in carborane and the fused ring (plane B) are 29.63 (8)º, 34.52 (10)º, and 36.14 (5)º, in comparison to smaller dihedral angles of 5.49 (8)º, 3.95 (7)º and 1.68 (4)º between planes B and C for **3n**, **4b**, and **5a**, respectively. Moreover, a certain degree of deformation of the *nido*-carborane unit was observed in **3n**, **4b**, and **5a** as the B11–C7 bonds (1.589 (4)–1.605 (4) Å, Figure 3) are shortened in comparison with those in ***nido*-1** and ***nido*-2** (1.629 (5) and 1.647 (2) Å, Figures 3 and S8). In the mid-rings (plane B), some bonds are also shortened (e.g. $d_{B11–C1}$ = 1.529 (4) Å for **3n** *vs* $d_{B–C}$ = 1.606 Å for the classical B–C single bond;[89] $d_{C3–C7}$= 1.468 (3) Å for **3n** *vs* $d_{C–C}$ = 1.54 Å for the classical C–C bond). These data indicate certain electronic delocalization for the fused system.

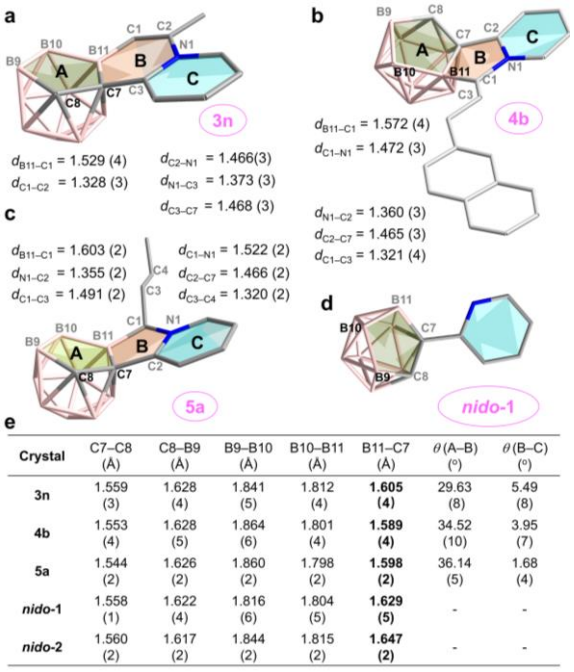

e

Crystal	C7–C8 (Å)	C8–B9 (Å)	B9–B10 (Å)	B10–B11 (Å)	B11–C7 (Å)	θ (A–B) (º)	θ (B–C) (º)
3n	1.559 (3)	1.628 (4)	1.841 (5)	1.812 (4)	**1.605 (4)**	29.63 (8)	5.49 (8)
4b	1.553 (4)	1.628 (5)	1.864 (6)	1.801 (4)	**1.589 (4)**	34.52 (10)	3.95 (7)
5a	1.544 (2)	1.626 (2)	1.860 (2)	1.798 (2)	**1.598 (2)**	36.14 (5)	1.68 (4)
nido-1	1.558 (1)	1.622 (4)	1.816 (6)	1.804 (5)	**1.629 (5)**	-	-
nido-2	1.560 (2)	1.617 (2)	1.844 (2)	1.815 (2)	**1.647 (2)**	-	-

Figure 3. Crystal structures of carborane-based tricyclic compounds (a) **3n**, (b) **4b**, (c) **5a**, and (d) control compound ***nido*-1**. Insets are the selected structural parameters for the middle ring (plane B) of carborane-based tricyclic compounds. e) The bond lengths and dihedral angles for the selected crystal structures. The estimated standard deviations values are shown in parentheses. The H atoms in crystal structures are omitted for clarity.

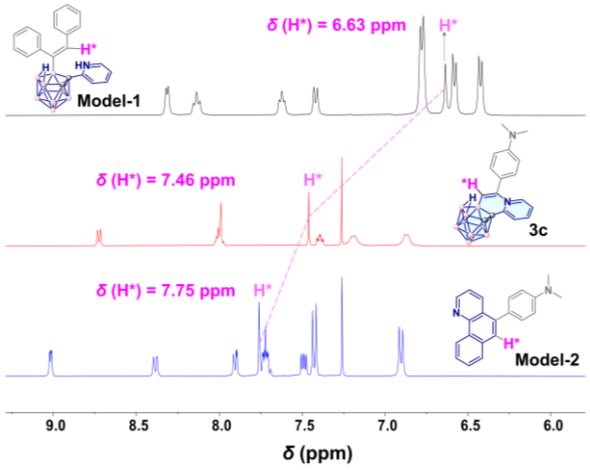

Figure 4. ^{1}H NMR spectra of **3c**, **Model-1**, and **Model-2**.

We also noticed that such a new fused system has an unprecedented downfield-shifted ^{1}H chemical shift (δ) for the olefinic CH in the fused six-membered ring (Figure 4). For example, the δ(H*) is 7.46 ppm for **3c**, but the olefinic CH proton in the non-fused compound **Model-1** (6.63 ppm) and other vinyl carborane derivatives[90–92] presents the range of 5.0–6.7 ppm. However, the δ(H*) in **3c** is similar to that value of the 2D aromatic **Model-2** (Figure 4). Quantum chemical calculations indicate that the downfield shifted δ(H*) in **3c** is caused by the diatropic ring current of the carborane cage (see Scheme 1 and details in the next section).

Theoretical calculations for boron cluster-cored tricyclics. Further insight into the above experimental findings has been obtained through quantum chemical calculations at the ZORA-BLYP(D3BJ)/TZ2P level of theory by means of the ADF software (see SI for further details on the computational method) on the set of compounds **3c**, **3n**, and **Model-1**–**Model-4** (see Figure 5). Computed equilibrium geometries are in good agreement with X-ray data (Figure S24 and Table S6). First, we have analyzed the aromaticity of these new fused compounds, with the aim to explain the above special electronic properties. For such, magnetic NICS, electronic MCI, and geometric HOMA criteria have been used on a set of compounds (Figure 5 and Figure S25). Once the fused system is obtained, both the 3D carborane and the 2D pyridyl ring remain aromatic. However, this is not the case with the newly formed ring between both entities. In particular, in the case of systems **3c** or **3n**, this new ring appears to be non-aromatic (MCI = 0.004, Figure 5), at difference to the equivalent ring in **Model-2**, which is weakly aromatic as expected from the Clar's π-sextet model (MCI = 0.017).[93, 94]

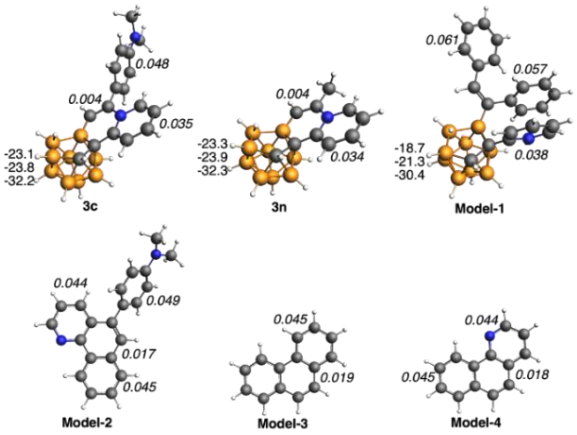

Figure 5. NICS (in ppm) for the top C_2B_3 ring, center of the cluster, and bottom B_5 ring of the carboranes, and MCI (in italics, in au) of the six-membered rings of the polycyclic aromatic hydrocarbons are included. For comparison, NICS for *nido*-$[C_2B_9H_{12}]^-$ are −22.0, −25.4 and −34.3 ppm, respectively, and for benzene is −7.4 ppm. As a reference, the MCI of benzene is 0.071 in au. Computed at the ZORA-BLYP(D3BJ)/TZ2P level of theory.

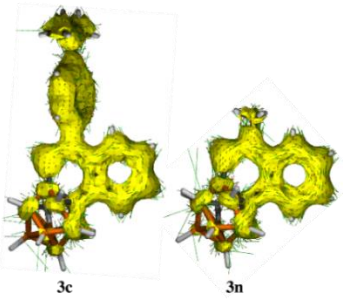

Figure 6. AICD plots (isosurface = 0.04) of compounds **3c** and **3n** (high-resolution pictures can be found in Figure S27).

The non-aromaticity of this mid-ring is further supported by HOMA (Figure S25). Geometrically, the localization of both the single and double bonds in this new ring also supports its non-aromaticity (Figure S26), despite a certain degree of delocalization, as stated above. And the latter agrees with the non-planarity of these systems as indicated by the X-ray data. Noticeably, the computed AICD plots allow us to observe how the ring current of this newly formed ring is interrupted (Figures 6 and S27). Thus, the hypothesized 2D-3D global aromaticity of these compounds does not take place, but aromaticity is localized on the 3D carborane and on the 2D pyridyl ring, not on the intermediate fused newly formed six-membered ring.[95, 96]#remove ref. 95 and change 95 by 14# Then, what is the reason for the distinct NMR properties of these systems? In particular, what is the origin of the unprecedented ^{1}H NMR chemical shift of 7.46 ppm for the H atom of the fused six-membered ring $\delta(H^*)$ of **3c**?

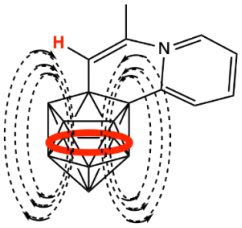

Scheme 1. Schematic representation of the coupling between the induced magnetic field created by the diatropic ring current of the carborane cage (ring in red) and the H atom of the fused ring (H in red) for system **3n**.

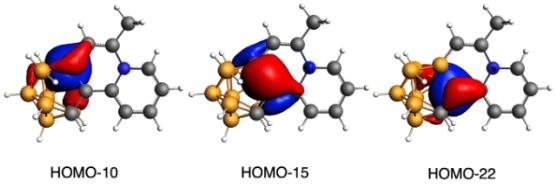

Figure 7. Localized molecular orbitals of system **3n** involving the delocalization between the cage of carborane and the aromatic ring.

To answer these questions, we have computed the chemical shift of compound **3n**, together with a series of derived model systems (Figure S28 and Table S5). These model compounds are aimed to understand if the ^{1}H NMR is either affected by the carborane or the newly formed pyridyl ring. The results allow attributing the downfield chemical shift to the ring current of the carborane (systems **3n^{I}**, **3n^{II}**, and **3n^{III}** in Figure S28). Indeed, as some of us have shown in previous work,[97]#remove ref. 97 and change 97 by 13# the ring currents of the *nido*-$[C_2B_9H_{12}]^-$ cluster are diatropic and quite intense. Moreover, we also found that the strongest diatropic ring current of the carborane is located in the middle of the two five-membered rings of the carborane, instead of the initially thought five-membered open face. These strong diatropic ring currents in the carborane unit generate an induced magnetic field that affects the ^{1}H NMR of the new fused six-membered ring (Scheme 1). The proton attached to this mid-ring is downfielded not because the ring is aromatic, but because of the induced magnetic field created by the carborane unit. This induced magnetic field is responsible for the experimental ^{1}H NMR chemical shift of 7.46 ppm for the H atom of the fused six-membered ring of **3c** (Figure 4). Then, although we can not talk about a fully aromatic system because of the non-aromaticity of either the five- or -six-membered ring between the carborane and the substituted pyridine, we do prove that the ring current of the 3D cage causes the ^{1}H NMR chemical shift to be downfielded. In addition, in this case, we have also found certain conjugation between the carborane cage and the aromatic ring through the shared atoms. This is supported by the canonical molecular orbitals (Figure S29) that are delocalized by nature, but also by the localized molecular orbitals (Figure 7) that are shared between the carborane unit and the fused six-membered ring. These orbitals prove the existence of some conjugation between the carborane and the fused six-membered ring. Such conjugation is also responsible for the

abnormal properties discussed in the next section for this new series of synthesized species.

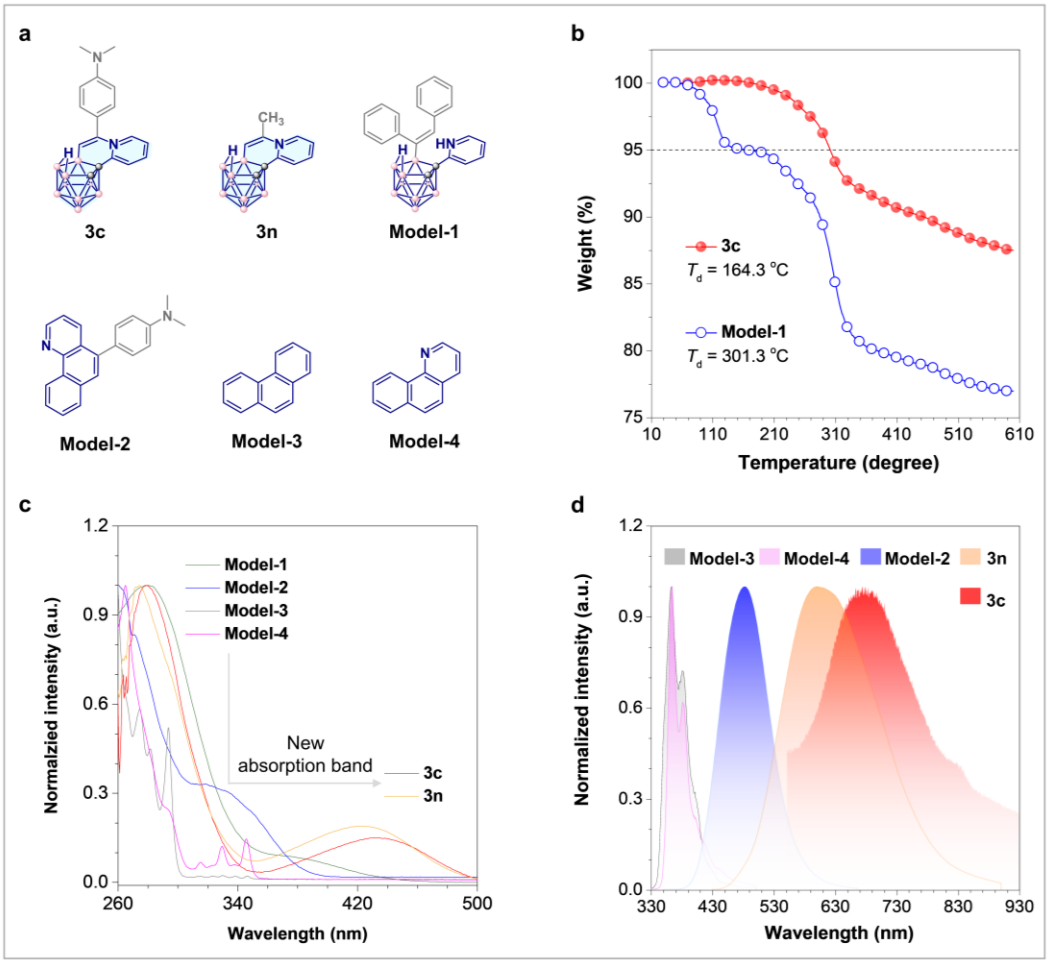

Figure 8. The study of the structure-property relationship with the selected compounds. a) The molecular structures of the selected compounds. b) Thermogravimetric analysis (TGA) for compounds **3c** and **Model-1**. c) The UV/Vis absorption spectra. d) The photoluminescence (PL) spectra for compounds **Model-2**, **Model-3**, **Model-4**, **3c**, and **3n** in THF solution (excitation wavelength = 420 nm for **3c** and **3n**, 280 nm for **Model-2**, **Model-3**, and **Model-4**).

The study of the physicochemical properties. It is well-known that the π conjugation effect in aromatic rings is an important structural parameter to determine the physicochemical properties of molecules. Owing to the unique conjugation effect between *nido*-carborane and the aromatic pyridine ring, one can expect new physicochemical properties. On the basis of this consideration, we chose **3c**, **3n**, and **Model-1** to **Model-4** to study the structure-property relationship (Figure 8).

The thermal stability of compounds **3c** and **Model-1** were first investigated by thermogravimetric analysis (TGA) at a heating rate of 10 °C/min under nitrogen (Figure 8b). The temperature of 5% weight loss (T_{d5}) for **3c** is 301 °C, which is much higher than that of the non-fused **Model-1** (160.3 °C). Obviously, the thermal stability is increased after the fusion between *nido*-carborane and aromatic ring, reflecting that the fused system contributes to the formation of a more stable system owing to the conjugation effect. This observation is also accorded with the findings in 2D systems where enhanced stability could be obtained if the whole conjugation of the molecule increases.

The UV-Vis spectra of **Model-2**, **Model-3**, **Model-4**, **3c**, and **3n** in THF were measured as shown in Figure 8c, among which **3c** and **3n** display a new absorption band centered at 431 and 422 nm, respectively, in contrast to control compounds **Model-1**–**Model-4**.[81] The generation of a new absorption band for carborane-fused compounds should be related to the electronic transition in the whole fused system. The UV-Vis spectra have also been obtained computationally (Figures S30 and S31), which demonstrate that the new absorption band corresponds to the HOMO → LUMO transition. Here both HOMO and LUMO orbitals involve the atoms of both the carborane and the new fused six-membered ring, further supporting the referred conjugation between the 3D and 2D entities. The PL spectra were performed as well (Figure 8d). **3c** and **3n** show the emission peaks at 675 and 602 nm, respectively, which is over 110 nm red shift than those of control compounds **Model-2**, **Model-3**, and **Model-4**. Thus, the carborane-fused systems considerably lower down the energy gap between the ground state and the excited state because of the unique conjugated structure. The photophysical properties of the boron cluster-cored compounds are significantly different from those of the 2D π-fused aromatic systems like **Model-2**–**Model-4**. Moreover, the carborane-fused molecular systems show large Stokes shift values beyond 7142 cm^{-1} (Table S3) and low quantum yields in solution(Φ < 1%, Table S4). The photoluminescence spectra of **3c** in different solvents demonstrate the solvatochromic effect (Figure S22). The

emission lifetimes range at a nanosecond level (Figure S23). These observations indicate that the emission arises from the intramolecular charge transfer state, where the carboranyl group acts as the electron donor while the pyridyl group behaves as an electron acceptor.[17, 30]

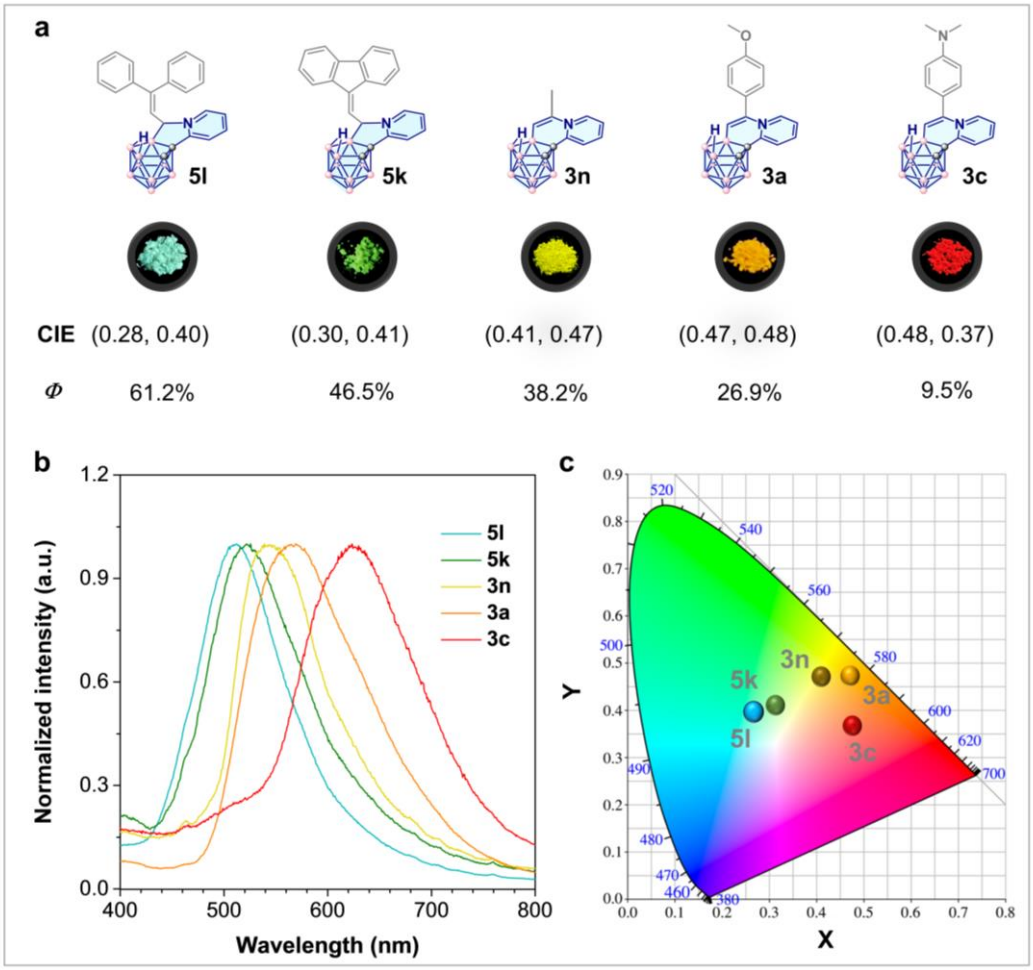

Figure 9. a) The selected carborane-based tricyclic compounds for solid-state emitters. Insets are the absolute luminescence efficiency in the solid state and CIE (Commission Internationale de l'Eclairage) coordinates. b) PL spectra in the solid state (excitation wavelength = 420 nm). c) CIE chromaticity coordinates.

Bright, color-tunable solid-state emitters. 2D π aromatics-based polycyclic systems have been widely utilized as building blocks for luminescent materials. However, their planar molecular structures usually have strong intermolecular interactions in the solid state, which may lead to the formation of non-emissive species such as exciplex, thus suffering from the aggregation-caused quenching effect.[98] Here, the bulk-sized 3D boron cluster-based tricyclic compounds may restrict the formation of the strong π···π interaction in the solid state, thus demonstrating efficient solid-state luminescence. To verify this point, the crystal packing structure of compound **3n** was selected as an example to analyze (Figure S9). Indeed, no π···π interaction was observed owing to the bulky and non-planar structure of the boron cluster-cored tricyclic compounds. Thus, bright solid-state emitters based on the above carborane-cored tricyclics are expected. Indeed, the color-tunable emissions have been realized from the selected boron cluster-cored structures through the change of the fused ring size and the substituent, as shown by the solid-state PL spectra (Figure 9b). The CIE coordinates can span the full range of visible light from blue to red (Figure 9c). To our delight, these fused structures demonstrate efficient solid-state efficiency (Φ) of up to 61.2% (Figure 9a). This is different from the 2D aromatic ring-fused systems, for example, *Rhodamine B* (Figure 1a), a commercially available dye that is non-emissive in the solid state.[99] The relatively low Φ of 9.5% for **3c** is related to the more facile non-radiative decay triggered by the smaller energy gap between the excited and ground states.[100, 101] These results indicate that the new hybrid conjugated systems might be the new-generation candidates for the solid-state emitters as they have evident advantages over the classical luminogens constructed fully by 2D aromatic rings.

CONCLUSION

We report a new molecular design for conjugation extension, denoted as fusion from a 2D aromatic ring and a 3D boron cluster. By virtue of this boron cage extension strategy, a library of boron cluster-cored tricyclic compounds with varying molecular skeletons could be quickly constructed based on one-pot Pd-catalyzed B–H activation and cascade annulation of *nido*-carboranes and N-heterocycles with alkynes. These new hybrid tricyclic molecular systems possess an unusual conjugation effect that determines excellent properties such as enhanced thermal stability, generation of new absorption bands, extremely red-shifted emissions (up to 230 nm), as well as tunable emissions covering

from blue to red with Φ up to 61% in the solid state. In sharp contrast, these properties are absent for the corresponding non-fused structures and classical 2D-fused aromatic systems. The present study provides a paradigm to rationally construct boron cluster-cored polycyclic molecules for potential applications.

ASSOCIATED CONTENT

Supporting Information. Materials and methods, synthetic procedures, characterization, crystallographic data and computational details, including Figures S1–S32 and Tables S1–S6. This material is available free of charge via the Internet at http://pubs.acs.org.

Corresponding Authors

*Deshuang Tu (tudeshuang@126.com)
*Jordi Poater (jordi.poater@ub.edu)
*Miquel Solà (miquel.sola@udg.edu)
*Hong Yan (hyan1965@nju.edu.cn)

ACKNOWLEDGMENT

This work was supported by the National Natural Science Foundation of China (21820102004 and 91961104), the Ministry of Science and Technology (2021YFE0114800), the Natural Science Foundation of Jiangsu Province (BZ2022007), the Ministerio de Ciencia e Innovación of Spain (PID2020-113711GB-I00, PID2019-106830GB-I00, MDM-2017-0767, and CEX2021-001202-M) and the Generalitat de Catalunya (2017SGR39). Excellent service by the Supercomputer center of the Consorci de Serveis Universitaris de Catalunya (CSUC) is gratefully acknowledged. High Performance Computing Center, Nanjing University and the Open Research Fund from Henan Normal University are also gratefully acknowledged. We are also grateful to Prof. Yong Liang for his helpful suggestions.

REFERENCES

(1) Ito, H.; Ozaki, K.; Itami, K., Annulative π-extension (APEX): Rapid access to fused arenes, heteroarenes, and nanographenes. *Angew. Chem. Int. Ed.* **2017,** *56*, 11144–11164.

(2) Türker, L.; Variş, S., A Review of polycyclic aromatic energetic materials. *Polycyclic Aromat. Compd.* **2009**, *29*, 228–266.

(3) Facchetti, A., π-Conjugated polymers for organic electronics and photovoltaic cell applications. *Chem. Mater.* **2011**, *23*, 733–758.

(4) von Grotthuss, E.; John, A.; Kaese, T.; Wagner, M., Doping polycyclic aromatics with boron for superior performance in materials science and catalysis. *Asian. J. Org. Chem.* **2018**, *7*, 37–53.

(5) Wang, Z.; Jiang, L.; Ji, J.; Zhou, F.; Lan, J.; You, J., Construction of cationic azahelicenes: Regioselective three-component annulation using in situ activation strategy. *Angew. Chem. Int. Ed.* **2020**, *59*, 23532–23536.

(6) Kang, M.; Zhang, Z.; Song, N.; Li, M.; Sun, P.; Chen, X.; Wang, D.; Tang, B. Z., Aggregation-enhanced theranostics: AIE sparkles in biomedical field. *Aggregate* **2020,** *1*, 80–106.

(7) AlZahrani, A., First-principles study on the structural and electronic properties of graphene upon benzene and naphthalene adsorption. *Appl. Surf. Sci.* **2010**, *257*, 807–810.

(8) Chen, F.; Tao, N., Electron transport in single molecules: from benzene to graphene. *Acc. Chem. Res.* **2009**, *42*, 429–438.

(9) Domenico, J.; Schneider, A. M.; Sohlberg, K., From benzene to graphene: Exploring the electronic structure of single-layer and bilayer graphene using polycyclic aromatic hydrocarbons. *J. Chem. Educ.* **2019**, *96*, 2225–2237.

(10) Grimes, R. N., *Carboranes*. Elsevier Science: 2016.

(11) Solà, M., Aromaticity rules. *Nat. Chem.* **2022**, *14*, 585–590.

(12) Poater, J.; Viñas, C.; Solà, M.; Teixidor, F., 3D and 2D aromatic units behave like oil and water in the case of benzocarborane derivatives. *Nat. Commun.* **2022,** *13*, 3844.

(13) Poater, J.; Viñas, C.; Bennour, I.; Escayola, S.; Solà, M.; Teixidor, F., Too Persistent to Give Up: Aromaticity in Boron Clusters Survives Radical Structural Changes. *J. Am. Chem. Soc.* **2020,** *142*, 9396–9407.

(14) Poater, J.; Viñas, C.; Olid, D.; Solà, M.; Teixidor, F., Aromaticity and extrusion of benzenoids linked to [*o*-COSAN]$^-$: Clar has the answer. *Angew. Chem. Int. Ed.* **2022,** *61*, e202200672.

(15) Bregadze, V. I., Dicarba-*closo*-dodecaboranes $C_2B_{10}H_{12}$ and their Derivatives. *Chem. Rev.* **1992**, *92*, 209–223.

(16) Mukherjee, S.; Thilagar, P., Boron clusters in luminescent materials. *Chem. Commun.* **2016**, *52*, 1070–1093.

(17) Ochi, J.; Tanaka, K.; Chujo, Y., Recent progress in the development of solid-state luminescent *o*-carboranes with stimuli responsivity. *Angew. Chem. Int. Ed.* **2020**, *59*, 9841–9855.

(18) Fisher, S. P.; Tomich, A. W.; Lovera, S.; Kleinsasser, J. F.; Guo, J.; Asay, M.; Nelson, H.; Lavallo, V., Nonclassical applications of *closo*-carborane anions: from main group chemistry and catalysis to energy storage. *Chem. Rev.* **2019**, *119*, 8262–8290.

(19) Núñez, R.; Tarrés, M.; Ferrer-Ugalde, A.; de Biani, F. F.; Teixidor, F., Electrochemistry and photoluminescence of icosahedral carboranes, boranes, metallacarboranes, and their derivatives. *Chem. Rev.* **2016**, *116*, 14307–14378.

(20) Ochi, J.; Yuhara, K.; Tanaka, K.; Chujo, Y., Controlling the dual-emission character of aryl-modified *o*-carboranes by intramolecular CH···O interaction sites. *Chem. Eur. J.* **2022,** *28*, e202200155.

(21) Li, X.; Yan, H.; Zhao, Q., Carboranes as a tool to tune phosphorescence. *Chem-Eur J* **2016**, *22*, 1888–1898.

(22) Dash, B. P.; Satapathy, R.; Gaillard, E. R.; Maguire, J. A.; Hosmane, N. S., Synthesis and properties of carborane-appended C_3-symmetrical extended π systems. *J. Am. Chem. Soc.* **2010**, *132*, 6578–6587.

(23) Spokoyny, A. M.; Machan, C. W.; Clingerman, D. J.; Rosen, M. S.; Wiester, M. J.; Kennedy, R. D.; Stern, C. L.; Sarjeant, A. A.; Mirkin, C. A., A coordination chemistry dichotomy for icosahedral carborane-based ligands. *Nat. Chem.* **2011**, *3*, 590–596.

(24) Messina, M. S.; Graefe, C. T.; Chong, P.; Ebrahim, O. M.; Pathuri, R. S.; Bernier, N. A.; Mills, H. A.; Rheingold, A. L.; Frontiera, R. R.; Maynard, H. D., Carborane RAFT agents as tunable and functional molecular probes for polymer materials. *Poly. Chem.* **2019**, *10*, 1660–1667.

(25) Hablot, D.; Ziessel, R.; Alamiry, M. A. H.; Bahraidah, E.; Harriman, A., Nanomechanical properties of molecular-scale bridges as visualised by intramolecular electronic energy transfer. *Chem. Sci.* **2013**, *4*, 444–453.

(26) Hosmane, N. S., *Boron science. New Technologies and Applications.* CRC Press: Boca Raton, **2011**.

(27) Wang, Q.-Y.; Wang, J.; Wang, S.; Wang, Z.-Y.; Cao, M.; He, C.-L.; Yang, J.-Q.; Zang, S.-Q.; Mak, T. C. W., *o*-Carborane-based and atomically precise metal clusters as hypergolic materials. *J. Am. Chem. Soc.* **2020**, *142*, 12010–12014.

(28) Liu, K.; Shang, C.; Wang, Z.; Qi, Y.; Miao, R.; Liu, K.; Liu, T.; Fang, Y., Non-contact identification and differentiation of illicit drugs using fluorescent films. *Nat. Commun.* **2018,** *9*, 1–11.

(29) Wang, Z.; Gou, X.; Shi, Q.; Liu, K.; Chang, X.; Wang, G.; Xu, W.; Lin, S.; Liu, T.; Fang, Y., Through-space charge transfer: a new way to develop a high-performance fluorescence sensing film towards opto-electronically inert alkanes. *Angew. Chem. Int. Ed.* **2022**, *61*, e202207619.

(30) Nghia, N. V.; Jana, S.; Sujith, S.; Ryu, J. Y.; Lee, J.; Lee, S. U.; Lee, M. H., *nido*-Carboranes: Donors for thermally activated delayed fluorescence. *Angew. Chem. Int. Ed.* **2018**, *57*, 12483–12488.

(31) Sun, J.; Gao, M.; Zhao, L.; Zhao, Y.; Li, T.; Chen, K.; Hu, X.; He, L.; Huang, Q.; Liu, M., Recent advances in carborane-siloxane polymers. *React. Funct. Polym.* **2022**, *173*, 105213.

(32) Fisher, S. P.; Tomich, A. W.; Lovera, S. O.; Kleinsasser, J. F.; Guo, J.; Asay, M. J.; Nelson, H. M.; Lavallo, V., Nonclassical applications of *closo*-carborane anions: from main group chemistry and catalysis to energy storage. *Chem. Rev.* **2019**, *119*, 8262–8290.

(33) Gruzdev, D. A.; Levit, G. L.; Krasnov, V. P.; Charushin, V. N., Carborane-containing amino acids and peptides: Synthesis, properties and applications. *Coord. Chem. Rev.* **2021,** *433*, 213753.

(34) Zhang, K.; Song, R.; Qi, J.; Zhang, Z.; Zhang, Z.; Yu, C.; Li, K.; Zhang, Z.; Li, B., Colossal barocaloric effect in carboranes as a performance tradeoff. *Adv. Funct. Mater.* **2022**, *32*, 2112622.

(35) Hosmane, N. S.; Eagling, R. D., *Handbook of boron science: with applications in organometallics, catalysis, materials and medicine (In 4 Volumes)*. World Scientific: London, **2018**.

(36) Hawthorne, M. F., The role of chemistry in the development of boron neutron capture therapy of cancer. *Angew. Chem. Int. Ed.* **1993**, *32*, 950–984.
(37) *Boron-based compounds: Potential and emerging applications in medicine*. Hey-Hawkins, E.; Viñas, C., Eds., Wiley: Chichester, **2018**.
(38) Issa, F.; Kassiou, M.; Rendina, L. M., Boron in drug discovery: carboranes as unique pharmacophores in biologically active compounds. *Chem. Rev.* **2011**, *111*, 5701–5722.
(39) Barry, N. P. E.; Sadler, P. J., Dicarba-*closo*-dodecarborane-containing half-sandwich complexes of ruthenium, osmium, rhodium and iridium: biological relevance and synthetic strategies. *Chem. Soc. Rev.* **2012**, *41*, 3264–3279.
(40) Hosmane, N. S., Maguire, J. A.; Zhu, Y.; Takagaki, M. *Future Perspectives for Boron and gadolinium neutron capture therapies in cancer treatment.* World Scientific: Singapore, Chapter 9, **2011**, 165–170.
(41) Stockmann, P.; Gozzi, M.; Kuhnert, R.; Sárosi, M. B.; Hey-Hawkins, E., New keys for old locks: Carborane-containing drugs as platforms for mechanism-based therapies. *Chem. Soc. Rev.* **2019**, *48*, 3497–3512.
(42) Yin, Y.; Ochi, N.; Craven, T. W.; Baker, D.; Takigawa, N.; Suga, H., De Novo carborane-containing macrocyclic peptides targeting human epidermal growth factor receptor. *J. Am. Chem. Soc.* **2019**, *141*, 19193–19197.
(43) Hu, K.; Yang, Z.; Zhang, L.; Xie, L.; Wang, L.; Xu, H.; Josephson, L.; Liang, S. H.; Zhang, M.-R., Boron agents for neutron capture therapy. *Coord. Chem. Rev.* **2020**, *405*, 213139.
(44) Scholz, M.; Hey-Hawkins, E., Carbaboranes as pharmacophores: properties, synthesis, and application strategies. *Chem. Rev.* **2011**, *111*, 7035–7062.
(45) Couto, M.; Mastandrea, I.; Cabrera, M.; Cabral, P.; Teixidor, F.; Cerecetto, H.; Viñas, C., Small-molecule kinase-inhibitors-loaded boron cluster as hybrid agents for glioma-cell-targeting therapy. *Chem-Eur J* **2017**, *23*, 9233–9238.
(46) Li, J.; Sun, Q.; Lu, C.; Xiao, H.; Guo, Z.; Duan, D.; Zhang, Z.; Liu, T.; Liu, Z., Boron encapsulated in a liposome can be used for combinational neutron capture therapy. *Nat. Commun.* **2022**, *13*, 1–11.
(47) Cígler, P.; Kožíšek, M.; Řezáčová, P.; Brynda, J.; Otwinowski, Z.; Pokorná, J.; Plešek, J.; Grüner, B.; Doležková-Marešová, L.; Máša, M.; Sedláček, J.; Bodem, J.; Kräusslich, H.-G.; Král, V.; Konvalinka, J., From nonpeptide toward noncarbon protease inhibitors: metallacarboranes as specific and potent inhibitors of HIV protease. *Proc. Nat. Acad. Sci.* **2005**, *102*, 15394–15399.
(48) Nuez-Martinez, M.; Pinto, C. I. G.; Guerreiro, J. F.; Mendes, F.; Marques, F.; Muñoz-Juan, A.; Xavier, J. A.; Laromaine, A.; Bitonto, V.; Protti, N.; Crich, S. G.; Teixidor, F.; Viñas, C. Cobaltabis(dicarbollide) ([*o*-COSAN]$^-$;) as multifunctional chemotherapeutics: a prospective application in boron neutron capture therapy (BNCT) for glioblastoma. *Cancers* **2021**. 13, 6367.
(49) Krebs, J.; Häfner, A.; Fuchs, S.; Guo, X.; Rauch, F.; Eichhorn, A.; Krummenacher, I.; Friedrich, A.; Ji, L.; Finze, M.; Lin, Z.; Braunschweig, H.; Marder, T. B., Backbone-controlled LUMO energy induces intramolecular C–H activation in ortho-bis-9-borafluorene-substituted phenyl and *o*-carboranyl compounds leading to novel 9,10-diboraanthracene derivatives. *Chem. Sci.* **2022,** *13*, 14165–14178.
(50) Krebs, J.; Haehnel, M.; Krummenacher, I.; Friedrich, A.; Braunschweig, H.; Finze, M.; Ji, L.; Marder, T. B., Synthesis and structure of an *o*-carboranyl-substituted three-coordinate borane radical anion. *Chem.-Eur. J.* **2021,** *27*, 8159–8167.
(51) Ji, L.; Riese, S.; Schmiedel, A.; Holzapfel, M.; Fest, M.; Nitsch, J.; Curchod, B. F. E.; Friedrich, A.; Wu, L.; Al Mamari, H. H.; Hammer, S.; Pflaum, J.; Fox, M. A.; Tozer, D. J.; Finze, M.; Lambert, C.; Marder, T. B., Thermodynamic equilibrium between locally excited and charge-transfer states through thermally activated charge transfer in 1-(pyren-2′-yl)-o-carborane. *Chem. Sci.* **2022,** *13*, 5205–5219.
(52) Zhang, C.; Liu, X.; Wang, J.; Ye, Q., A three-dimensional inorganic analogue of 9,10-diazido-9,10-diboraanthracene: a Lewis superacidic azido borane with reactivity and stability. *Angew. Chem. Int. Ed.* **2022,** *61*, e202205506.
(53) Yruegas, S.; Axtell, J. C.; Kirlikovali, K. O.; Spokoyny, A. M.; Martin, C. D., Synthesis of 9-borafluorene analogues featuring a three-dimensional 1,1′-bis(o-carborane) backbone. *Chem. Commun.* **2019,** *55*, 2892–2895.
(54)T. B. Marder, Ph.D. Thesis, University of California at Los Angeles, **1981**.
(55) Wilczynski, R.; Sneddon, L. G., Transition-metal-promoted reactions of boron hydrides. 2. synthesis and thermolysis reactions of alkenylpentaboranes. new synthesis of monocarbon carboranes. *Inorg. Chem.* **1981,** *20*, 3955–3962.
(56) Davan, T.; Corcoran, E. W., Jr.; Sneddon, L. G., Transition-metal-promoted reactions of boron hydrides. 5. Palladium-catalyzed pentaborane(9)-olefin coupling reactions: a new, mild synthetic route to alkenylpentaboranes. *Organometallics* **1983,** *2*, 1693–1694.
(57) Hewes, J. D.; Kreimendahl, C. W.; Marder, T. B.; Hawthorne, M. F., Metal-promoted insertion of an activated alkene into a boron-hydrogen bond of an exopolyhedral *nido*-rhodacarborane: rhodium-catalyzed hydroboration. *J. Am. Chem. Soc.* **1984,** *106*, 5757–5759.
(58) Mirabelli, M. G. L.; Sneddon, L. G., Transition-metal-promoted reactions of boron hydrides. 9. Cp*Ir-catalyzed reactions of polyhedral boranes and acetylenes. *J. Am. Chem. Soc.* **1988**, *110*, 449–453.
(59) Molinos, E.; Brayshaw, S. K.; Kociok-Köhn, G.; Weller, A. S., Sequential dehydrogenative borylation/hydrogenation route to polyethyl-substituted, weakly coordinating carborane anions. *Organometallics* **2007,** *26*, 2370–2382.
(60) Zhang, R.; Zhu, L.; Liu, G.; Dai, H.; Lu, Z.; Zhao, J.; Yan, H., Cobalt-promoted B–H and C–H activation: Facile B–C coupling of carboranedithiolate and cyclopentadienyl. *J. Am. Chem. Soc.* **2012**, *134*, 10341–10344.
(61) Wang, Z.; Ye, H.; Li, Y.; Li, Y.; Yan, H., Unprecedented boron-functionalized carborane derivatives by facile and selective cobalt-induced B–H activation. *J. Am. Chem. Soc.* **2013**, *135*, 11289–11298.
(62) Qiu, Z.; Quan, Y.; Xie, Z., Palladium-catalyzed selective fluorination of *o*-carboranes. *J. Am. Chem. Soc.* **2013,** *135*, 12192–12195.
(63) Yao, Z.-J.; Yu, W.-B.; Lin, Y.-J.; Huang, S.-L.; Li, Z.-H.; Jin, G.-X., Iridium-mediated regioselective B–H/C–H activation of carborane cage: a facile synthetic route to metallacycles with a carborane backbone. *J. Am. Chem. Soc.* **2014**, *136*, 2825–2832.
(64) Quan, Y.; Xie, Z., Iridium catalyzed regioselective cage boron alkenylation of *o*-carboranes via direct cage B–H activation. *J. Am. Chem. Soc.* **2014**, *136*, 15513–15516.
(65) Dziedzic, R. M.; Saleh, L. M. A.; Axtell, J. C.; Martin, J. L.; Stevens, S. L.; Royappa, A. T.; Rheingold, A. L.; Spokoyny, A. M., B–N, B–O, and B–CN bond formation *via* palladium-catalyzed cross-coupling of B-bromo-carboranes. *J. Am. Chem. Soc.* **2016**, *138*, 9081–9084.
(66) Zhang, Y.; Sun, Y.; Lin, F.; Liu, J.; Duttwyler, S., Rhodium(III)-catalyzed alkenylation–annulation of *closo*-dodecaborate anions through double B−H activation at room temperature. *Angew. Chem. Int. Ed.* **2016**, *55*, 15609–15614.
(67) Zhang, X.; Zheng, H.; Li, J.; Xu, F.; Zhao, J.; Yan, H., Selective catalytic B–H arylation of *o*-carboranyl aldehydes by a transient directing strategy. *J. Am. Chem. Soc.* **2017**, *139*, 14511–14517.
(68) Lin, F.; Yu, J.-L.; Shen, Y.; Zhang, S.-Q.; Spingler, B.; Liu, J.; Hong, X.; Duttwyler, S., Palladium-catalyzed selective five-fold cascade arylation of the 12-vertex monocarborane anion by B–H activation. *J. Am. Chem. Soc.* **2018**, *140*, 13798–13807.
(69) Yang, Z.; Zhao, W.; Liu, W.; Wei, X.; Chen, M.; Zhang, X.; Zhang, X.; Liang, Y.; Lu, C.; Yan, H., Metal-free oxidative B−N coupling of *nido*-carborane with N-heterocycles. *Angew. Chem. Int. Ed.* **2019**, *58*, 11886–11892.
(70) Shen, Y.; Zhang, K.; Liang, X.; Dontha, R.; Duttwyler, S., Highly selective palladium-catalyzed one-pot, five-fold B–H/C–H cross coupling of monocarboranes with alkenes. *Chem. Sci.* **2019**, *10*, 4177–4184.
(71) Baek, Y.; Cheong, K.; Ko, G. H.; Han, G. U.; Han, S. H.; Kim, D.; Lee, K.; Lee, P. H., Iridium-catalyzed cyclative indenylation and dienylation through sequential B(4)–C bond formation, cyclization, and elimination from *o*-carboranes and propargyl alcohols. *J. Am. Chem. Soc.* **2020**, *142*, 9890–9895.
(72) Mills, H. A.; Martin, J. L.; Rheingold, A. L.; Spokoyny, A. M., Oxidative generation of boron-centered radicals in carboranes. *J. Am. Chem. Soc.* **2020,** *142*, 4586–4591.
(73) Cheng, R.; Zhang, J.; Zhang, H.; Qiu, Z.; Xie, Z., Ir-catalyzed enantioselective B−H alkenylation for asymmetric synthesis of chiral-at-cage *o*-carboranes. *Nat. Commun.* **2021**, *12*, 7146.
(74) Chen, M.; Zhao, D.; Xu, J.; Li, C.; Lu, C.; Yan, H., Electrooxidative B−H functionalization of *nido*-carboranes. *Angew. Chem. Int. Ed.* **2021**, *60*, 7838–7844.

(75) Cao, K.; Xu, T.-T.; Wu, J.; Zhang, C.-Y.; Wen, X.-Y.; Yang, J., The in situ NHC-palladium catalyzed selective activation of B(3)–H or B(6)–H bonds of *o*-carboranes for hydroboration of alkynes: An efficient approach to alkenyl-*o*-carboranes. *Inorg. Chem.* **2021**, *60*, 1080–1085.

(76) Yang, L.; Bongsuiru Jei, B.; Scheremetjew, A.; Kuniyil, R.; Ackermann, L., Electrochemical B−H nitrogenation: access to amino acid and BODIPY-labeled *nido*-carboranes. *Angew. Chem. Int. Ed.* **2021**, *60*, 1482–1487.

(77) Qiu, Z.; Xie, Z., A Strategy for selective catalytic B–H functionalization of *o*-carboranes. *Acc. Chem. Res.* **2021**, *54*, 4065–4079.

(78) Cui, P.-F.; Liu, X.-R.; Guo, S.-T.; Lin, Y.-J.; Jin, G.-X., Steric-effects-directed B–H bond activation of *para*-carboranes. *J. Am. Chem. Soc.* **2021**, *143*, 5099–5105.

(79) Fu, Y.; Li, Y.; Luo, D.; Lu, Y.; Huang, J.; Yang, Z.; Lu, J.; Jiang, Y.-Y.; Lu, J.-Y., Palladium-catalyzed regioselective B(3,4)–H acyloxylation of *o*-carboranes. *Inorg. Chem.* **2022**, *61*, 911–922.

(80) Ma, Y.-N.; Gao, Y.; Ma, Y.; Wang, Y.; Ren, H.; Chen, X., Palladium-catalyzed regioselective B(9)-amination of *o*-carboranes and *m*-carboranes in HFIP with broad nitrogen sources. *J. Am. Chem. Soc.* **2022**, *144*, 8371–8378.

(81) Sun, F.; Tan, S.; Cao, H.-J.; Xu, J.; Bregadze, V. I.; Tu, D.; Lu, C.; Yan, H., Palladium-catalyzed hydroboration of alkynes with carboranes: Facile construction of a library of boron cluster-based AIE-active luminogens. *Angew. Chem. Int. Ed.* **2022**, 61, e202207125.

(82) Al-Masum, M.; Meguro, M.; Yamamoto, Y., The two component palladium catalyst system for intermolecular hydroamination of allenes. *Tetrahedron Lett.* **1997**, *38*, 6071–6074.

(83) Warratz, S.; Kornhaaß, C.; Cajaraville, A.; Niepötter, B.; Stalke, D.; Ackermann, L., Ruthenium(II)-catalyzed C–H activation/alkyne annulation by weak coordination with O_2 as the sole oxidant. *Angew. Chem. Int. Ed.* **2015**, *54*, 5513–5517.

(84) Mather, B. D.; Viswanathan, K.; Miller, K. M.; Long, T. E., Michael addition reactions in macromolecular design for emerging technologies. *Prog. Polym. Sci.* **2006**, *31*, 487–531.

(85) Tejedor, D.; Méndez-Abt, G.; Cotos, L.; García-Tellado, F., Propargyl Claisen rearrangement: allene synthesis and beyond. *Chem. Soc. Rev.* **2013**, *42*, 458–471.

(86) Trost, B. M.; Weber, L.; Strege, P. E.; Fullerton, T. J.; Dietsche, T. J., Allylic alkylation: nucleophilic attack on π-allylpalladium complexes. *J. Am. Chem. Soc.* **1978**, *100*, 3416–3426.

(87) Murai, M.; Nishimura, K.; Takai, K., Palladium-catalyzed double-bond migration of unsaturated hydrocarbons accelerated by tantalum chloride. *Chem. Commun.* **2019**, *55*, 2769–2772.

(88) Cui, P.-F.; Liu, X.-R.; Lin, Y.-J.; Li, Z.-H.; Jin, G.-X., Highly selective separation of benzene and cyclohexane in a spatially confined carborane metallacage. *J. Am. Chem. Soc.* **2022**, *144*, 6558–6565.

(89) Allen, F. H.; Kennard, O.; Watson, D. G.; Brammer, L.; Orpen, A. G.; Taylor, R., Tables of bond lengths determined by X-ray and neutron diffraction. Part 1. Bond lengths in organic compounds. *J. Chem. Soc., Perkin Trans. 2* **1987**, S1–S19.

(90) Quan, Y.; Xie, Z., Palladium-catalyzed regioselective intramolecular coupling of *o*-carborane with aromatics *via* direct cage B–H activation. *J. Am. Chem. Soc.* **2015**, *137*, 3502–3505.

(91) Ni, H.; Lu, Z.; Xie, Z., Transition-metal-free cross-coupling reaction of iodocarboranes with terminal alkynes enabled by UV light: synthesis of 1-alkynyl-*o*-carboranes and carborane-fused cyclics. *J. Am. Chem. Soc.* **2020,** *142*, 18661–18667.

(92) Lyu, H.; Quan, Y.; Xie, Z., Palladium-catalyzed direct dialkenylation of cage B–H bonds in *o*-carboranes through cross-coupling reactions. *Angew. Chem. Int. Ed.* **2015**, *54*, 10623–10626.

(93) Clar, E., The aromatic sextet. Wiley, New York, **1972**.

(94) Solà, M., Forty years of Clar's aromatic π-sextet rule. *Front. Chem.* **2013**, *1*, 22.

(95) Poater, J.; Viñas, C.; Olid, D.; Solà, M.; Teixidor, F., Aromaticity and extrusion of benzenoids linked to [*o*-COSAN]⁻: Clar has the answer. *Angew. Chem. Int. Ed.* **2022**, *61*, e202200672. #remove ref. It is already ref. 14#

(96) Buzsáki, D.; Kovács, M. B.; Hümpfner, E.; Harcsa-Pintér, Z.; Kelemen, Z., Conjugation between 3D and 2D aromaticity: does it really exist? The case of carborane-fused heterocycles. *Chem. Sci.* **2022**, 13, 11388–11393.

(97) Poater, J.; Viñas, C.; Bennour, I.; Escayola, S.; Solà, M.; Teixidor, F., Too persistent to give up: Aromaticity in Boron clusters survives radical structural changes. *J. Am. Chem. Soc.* **2020**, *142*, 9396–9407.#remove ref. It is already ref. 13#

(98) Gao, M.; Tang, B. Z., AIE-based cancer theranostics. *Coord. Chem. Rev.* **2020,** *402*, 213076.

(99) Kamino, S.; Horio, Y.; Komeda, S.; Minoura, K.; Ichikawa, H.; Horigome, J.; Tatsumi, A.; Kaji, S.; Yamaguchi, T.; Usami, Y., A new class of rhodamine luminophores: design, syntheses and aggregation-induced emission enhancement. *Chem. Commun.* **2010**, *46*, 9013–9015.

(100) Siebrand, W., Radiationless transitions in polyatomic molecules. II. Triplet ‐ ground ‐ state transitions in aromatic hydrocarbons. *J. Chem. Phys.* **1967**, *47*, 2411–2422.

(101) Englman, R.; Jortner, J., The energy gap law for radiationless transitions in large molecules. *Mol. Phys.* **1970**, *18*, 145–164.

Insert Table of Contents artwork here